OPEN

Intravenous Bone Marrow Stem Cell Grafts Preferentially Migrate to Spleen and Abrogate Chronic Inflammation in Stroke

Sandra A. Acosta, PhD; Naoki Tajiri, PhD; Jaclyn Hoover, MS; Yuji Kaneko, PhD; Cesar V. Borlongan, PhD

Background and Purpose—Adult stem cell therapy is an experimental stroke treatment. Here, we assessed homing and anti-inflammatory effects of bone marrow stromal cells (hBMSCs) in chronic stroke.

Methods—At 60 days post stroke, adult Sprague–Dawley rats received intravenous hBMSCs (4×10^6 labeled or nonlabeled cells) or vehicle (saline). A sham surgery group served as additional control. In vivo imaging was conducted between 1 hour and 11 days post transplantation, followed by histological examination.

Results—Labeled hBMSCs migrated to spleen which emitted significantly higher fluorescent signal across all time points, especially during the first hour, and were modestly detected in the head region at the 12 hours and 11 days, compared with nonlabeled hBMSCs and vehicle-infused stroke animals, or sham ($P<0.05$). At 11 days post transplantation, ex vivo imaging confirmed preferential hBMSC migration to the spleen over the brain. Hematoxylin and eosin staining revealed significant 15% and 30% reductions in striatal infarct and peri-infarct area, and a trend of rescue against neuronal loss in the hippocampus. Unbiased stereology showed significant 75% and 60% decrements in major histocompatibility complex II–activated inflammatory cells in gray and white matter, and a 43% diminution in tumor necrosis factor-α cell density in the spleen of transplanted stroke animals compared with vehicle-infused stroke animals ($P<0.05$). Human antigen immunostaining revealed 0.03% hBMSCs survived in spleen and only 0.0007% in brain. MSC migration to spleen, but not brain, inversely correlated with reduced infarct, peri-infarct, and inflammation.

Conclusions—hBMSC transplantation is therapeutic in chronic stroke possibly by abrogating the inflammation-plagued secondary cell death. **(*Stroke*. 2015;46:2616-2627. DOI: 10.1161/STROKEAHA.115.009854.)**

Key Words: brain ischemia ■ inflammation ■ imaging ■ regeneration ■ stem cells

Stroke is a leading cause of death and the number one cause of disability in the United States,[1,2] with an estimated 795 000 new or recurrent stroke events annually, but with only 1 Food and Drug Administration–approved drug, namely tissue-type plasminogen activator.[1–4] Moreover, tissue-type plasminogen activator's therapeutic window is limited ≤4.5 hours after stroke onset because of the drug's accompanying complications, such as hemorrhagic transformation, when administered beyond this time period.[5,6] Finding a therapeutic intervention that would retard the progressive secondary neurodegeneration will benefit chronic stroke survivors missing the acute tissue-type plasminogen activator treatment. Stem cell–based therapy has emerged as a potential treatment for ischemic stroke. To date, most cell transplantation studies have been conducted on animals during acute time points post stroke injury, leaving chronic time points understudied.[7–11] Preclinical studies have demonstrated safety and efficacy of cell therapy in animal models of stroke,[12–15] with limited clinical trials providing solid safety and tolerability profile in stroke patients transplanted with human adult stem cells.[16–19]

The mechanism of action of stem cell transplantation remains not fully understood. The passive biodistribution and active homing migration patterns of grafted stem cells may provide insights into the cells' mechanism of action, which represents a major gap in our knowledge about stem cell therapy in stroke. Modulation of inflammatory pathways has been postulated as a robust strategy in altering the secondary cell death of the ischemic brain.[7,20] Inflammatory responses both intrinsic to brain and those derived from peripheral organ–specific infiltrating cells, including neutrophils, T cells, and monocytes/macrophages, mediate the secondary neurodegeneration seen in stroke.[21] Cell-based and pharmacological anti-inflammatory therapies have been shown to improve the stroke outcome.[22–26] Intravenously infused stem cells migrate to the spleen in acute stroke.[25] However, in chronic stroke, peripheral administration of cells is viewed as suboptimal

Received April 22, 2015; final revision received May 28, 2013; accepted June 9, 2015.

From the Center of Excellence for Aging and Brain Repair, Department of Neurosurgery and Brain Repair, University of South Florida College of Medicine, Tampa.

Correspondence to Cesar V. Borlongan, PhD, 12901 Bruce B. Downs Blvd, Tampa, FL 33612. E-mail cborlong@health.usf.edu

© 2015 The Authors. *Stroke* is published on behalf of the American Heart Association, Inc., by Wolters Kluwer. This is an open access article under the terms of the Creative Commons Attribution Non-Commercial-NoDervis License, which permits use, distribution, and reproduction in any medium, provided that the original work is properly cited, the use is noncommercial, and no modifications or adaptations are made.

***Stroke* is available at http://stroke.ahajournals.org** **DOI: 10.1161/STROKEAHA.115.009854**

because grafted cells do not penetrate well across the reconstituted blood–brain barrier, thereby necessitating the need for direct transplantation of cells into the peri-infarct areas of the ischemic brain. Here, we tested the hypothesis that despite failure of the majority of peripherally administered cells to reach the chronic stroke brain, the cells' potential to migrate to the spleen would likely be sufficient to attenuate splenic inflammatory response and might be effective enough to afford therapeutic benefits against stroke.

Materials and Methods

Subjects

All experiments were conducted in accordance with the National Institute of Health Guide and Use of Laboratory Animals and were approved by the Institutional Animal Care and Use Committee of the University of South Florida, Morsani College of Medicine. Rats were housed 2 per cage in a temperature- and humidity-controlled room that was maintained on 12/12-hour light/dark cycles. They had free access to food and water. All necessary steps were performed to minimize animal pain and stress throughout the study. Two-month-old Sprague–Dawley male rats (Harlan Laboratories, Indianapolis, IN) served as subjects and either exposed to sham or stroke surgery (n=15, representative of each treatment condition, were available).

Fluorescent Labeling of Cultured hBMSC Grafts

Human CD133+ cells were isolated from granulocyte-colony stimulating factor–mobilized leukapheresed blood using magnetic cell sorting technology. This use of human bone marrow cells was approved by the University Institutional Review Board. From the initial heterogeneous cell population, CD133+ cells constituted 1% to 2%, with the remainder being CD133− cells. Using the harvested CD133+ cell sample, flow cytometry revealed 75% to 85% purity for CD133+ antigens. Approximately, 87% of the selected CD133+ cells were viable on completion of the cell isolation process. CD133+ hBMSCs were then suspended (6.7×10^5 cells/T75 flask) in 10 mL of supplemented growth medium and grown in noncoated T-75 flasks at 37°C in humidified atmosphere containing 5% carbon dioxide. hBMSCs were grown until they were 90% confluent and then subcultured. For graft preparation, hBMSCs were harvested, and the cell density was adjusted as 4×10^6 cells in 500 μL of PBS. Thereafter, cells were incubated with XenoLight 1,1′-dioctadecyl-3,3,3′,3′-tetramethylindotricbocyanine iodide (DiR; catalog #125964; Caliper Life Sciences) for 30 minutes to evaluate migration of the transplanted hBMSCs. After the labeling, cells were rinsed using PBS and centrifuged twice. Finally, the pellet of labeled cells was suspended in 500 μL of PBS just before the transplantation.

Stroke Surgery

Stroke surgery was performed using the middle cerebral artery occlusion (MCAo) technique as described in our previous studies.[27] Animals were anesthetized with a mixture of 1% to 2% isoflurane in nitric oxide/oxygen (69%/30%) via a face mask, and body temperature was maintained at 37±0.3°C during the surgical procedures. A midline skin incision was made in the neck with subsequent exploration of the left common carotid artery, the external carotid artery, and internal carotid artery. Thereafter, a 4-0 monofilament nylon suture (27.0–28.0 mm) was advanced from the common carotid artery bifurcation until it blocked the origin of the MCA. Animals were allowed to recover from anesthesia during MCAo. Hours after MCAo, animals were reanesthetized and reperfused by withdrawal of the nylon thread. We have standardized the MCAo model, with stroke animals showing ≥80% reduction in regional cerebral blood flow during the occlusion period as determined by laser Doppler (Perimed). We also found no significant differences in physiological parameters, including Pao_2, $PaCO_2$, and plasma pH measurements, in our stroke animals indicating similar degree of stroke insults. Rats that reached the 80% cerebral blood flow reduction during occlusion were used for future studies. Sham animals were also included in this study, which involved anesthetizing rats and making an incision in the neck area, then exposing and isolating the common carotid and internal carotid arteries, ligating the external carotid artery, but without inserting the filament. Thereafter, incisions were closed and animals were allowed to recover from anesthesia. All animals were euthanized at 71 days post MCAo for subsequent imaging analysis.

Intravenous Administration of hBMSCs

After 60 days post stroke surgery, animals were anesthetized with 1% to 2% isoflurane in nitrous oxide/oxygen (69%/30%) using a face mask. hBMSCs-DiR+ (4×10^6 DiR-labeled cells in 500 μL of sterile saline), hBMSCs-DiR− (4×10^6 nonlabeled viable cells in 500 μL of sterile saline), or saline (vehicle; 500 μL of sterile saline 0.9% NaCl) were administered via the jugular vein. Animals were euthanized 11 days post transplantation and transcardially perfused with saline and 4% paraformaldehyde.

XenoLight DiR for In Vivo and Ex Vivo Biodistribution Imaging Procedures

Sprague–Dawley rats received MCAo surgery. After 60 days post MCAo, ≈4×10^6 viable hBMSC-DiR+ cells (DiR-labeled), hBMScs-DiR− (DiR-nonlabeled), and saline (500 μL of cold sterile saline) were infused into the jugular vein. To visualize DiR fluorescence emitted from the engrafted hBMSCs in vivo, the head and abdomen of the animals were shaved to avoid light scattering, and the animals were anesthetized in a chamber with 3.0% isoflurane. Once the rats were completely anesthetized, the animals were transferred from the chamber to the IVIS Spectrum 200 Imaging System (Xenogen), and the isoflurane level was set at 1% to 2% until complete image acquisition. The biodistribution of DiR-labeled hBMSCs grafts was monitored at 1, 4, 12, 24, 48, and 72 hours and day 11 after transplantation. Rats were imaged ventrally at all time points. A second set of images were obtained for the head region using a higher magnification. Identical illumination parameters (exposure time=auto; lamp voltage=high; f/stop=2; field of view=B [for head] and C [for whole body]; binning=8; emission filter=800 nm; and excitation filter=745 nm) were selected for all acquisition. All captured images were analyzed with Living Image software 4.0 (Xenogen). To analyze the change in DiR fluorescence intensity, identical regions of interest were placed on the abdomen and head area for animals. The same region of interest was also placed on the control animal as the background reference. Background efficiency was subtracted from each of the individual animal's efficiency and presented as an average radiant efficiency (photons per second per square centimeter per steridian divided by microwatts per square centimeter).

Brain and Organ Harvesting, Fixation, and Sectioning

Under deep anesthesia, rats were euthanized on day 11 post transplantation for ex vivo imaging analysis. Briefly, animals were perfused through the ascending aorta with 200 mL of cold PBS, followed by 200 mL of 4% paraformaldehyde in PB. Brains, spleen, lungs, and liver were removed and postfixed in the same fixative for 24 hours, followed by 30% sucrose in PB until completely sunk. Series of coronal sections were cut at a thickness of 40 μm with a cryostat and stored at −20°C.

Measurement of Infarct and Peri-Infarct Area

Hematoxylin and eosin staining was performed to confirm the core infarct injury of our stroke model. As shown in our previous studies,[28–30] we also demonstrated here that the primary damage produced by MCAo model was to subcortical areas, including the striatum and the hippocampus. Six coronal sections between the anterior edge and posterior edge of the infarcted striatum area were collected and processed for hematoxylin and eosin staining from each brain perfused at day 11 post transplantation. Sections were

cut at a thickness of 40 μm by cryostat. Every sixth coronal tissue section, beginning at anteroposterior (AP) +2.0 mm and ending at AP −3.8 mm posterior from bregma,[31] was randomly selected for measurement of infarct and peri-infarct area. Brain sections were examined using a light microscope (Olympus) and Keyence microscope (Keyence). The infarct area of brain damage was measured in each slice and quantified by a computer-assisted image analysis system (NIH Image Software) and calculated by the following formula: ([area of the damaged region in each section]×0.040) (mm^3). The peri-infarct area of brain damage was counted by a computer-assisted image analysis system (NIH Image Software). Infarct and peri-infarct areas were then expressed as a percentage of the ipsilateral hemisphere compared with the contralateral hemisphere. Scores for infarct lesion were rated accordingly: low <30%, medium 30% to 60%, and high >60%.

Measurement of Hippocampal Cell Loss

Cell loss revealed by hematoxylin and eosin staining was also analyzed in hippocampal CA1 and CA3 area to cover the entire vulnerable areas of the hippocampus after ischemic injury in our model of chronic stroke. Starting at coordinates AP −1.7 mm and ending AP-3.8 mm from bregma,[31] coronal brain sections (40 μm) collected covering the whole dorsal hippocampus. A total number of 6 sections per rat were used. Cells presenting with nuclear and cytoplasmic staining (hematoxylin and eosin) were manually counted in the CA1 and CA3 neurons. Cell count region of interest spanned the whole CA1 and CA3 areas in both the ipsilateral and contralateral side. Sections were examined with Nikon Eclipse 600 microscope at ×20. All data represented as mean values with ±SEM were then expressed as a percentage of the ipsilateral hemisphere compared with the contralateral hemisphere.

Major Histocompatibility Complex II Staining

Adaptive immunity is mediated by T cells, with T helper (Th) 1 and Th2 representing the classical proinflammatory and the alternative anti-inflammatory response of T cells, respectively. Each T-cell subset (Th1 or Th2) represents a specific pathway whereby distinct effector cells or proteins would instigate a different response. For instance, the main effectors of Th1 immunity are activated macrophages (M1), microglia cells (MHCII+), CD8+T cells, B cells, and interferon-γ altogether instigating an inflammatory response to injury. The present immunostaining focused on characterizing this Th1/M1 proinflammatory response using MHCII+ cells as markers of inflammation. Staining for major histocompatibility complex II (MHCII) cells (via OX6) was conducted on every 1 of 6 coronal section throughout the brain; coordinates AP +2.0 to AP −4.56.[31] In all animals, sections were anatomically matched. Series of 6 sections per rat were processed for MHCII staining. Six free-floating coronal sections (40 μm) were washed 3× in 0.1 mol/L PBS to clean the section from the cryoprotectant. Afterward, all sections were incubated in 2% hydrogen peroxide (H_2O_2) solution for 20 minutes and washed 3× with PBS for 10 minutes each wash. Next, all sections were incubated in blocking solution for 1 hour using PBS supplemented with 5% normal goat serum and 0.1% Triton X-100. Sections were then incubated overnight at 4°C with goat anti-OX6 (MHC or MHCII; 1:750 BD), antibody markers in PBS supplemented with 3% normal serum and 0.1% triton X-100. Sections were then washed 3× with PBS and incubated in biotinylated horse anti-goat secondary antibody (1:200; Vector Laboratories, Burlingame, CA) in PBS supplemented with normal horse serum, and 0.1% Triton X-100 for 1 hour. Next, the sections were incubated for 60 minutes in avidin–biotin substrate (ABC kit, Vector Laboratories, Burlingame, CA) and washed 3× with PBS for 10 minute each wash. All sections were then incubated for 1 minute in 3, 30-diaminobenzidine (DAB) with metal enhancer (Vector Laboratories) and washed 3× with PBS for 10 minutes each wash. Sections were then mounted onto glass slides, dehydrated in ascending ethanol concentration (70%, 95%, and 100%) for 2 minutes each and 2 minutes in xylenes, and cover-slipped using mounting medium.

Tumor Necrosis Factor-α Staining and Analysis

Staining for tumor necrosis factor-α (TNF-α) positive cells was conducted on every 1 of 6 sections, 20 mm thick, spanning the entire red pulp of the spleen. Free-floating sections were washed 3× for 5 minutes in PBS. For TNF-α staining, spleen sections were incubated with saline sodium citrate solution at pH 6 for 40 minutes at 80°C for antigen retrieval. Then, samples were blocked for 60 minutes at room temperature with 8% normal goat serum (Invitrogen, CA) in PBS containing 0.1% Tween 20 (PBST; Sigma). Sections were then incubated overnight at 4°C with rabbit polyclonal anti-TNF-α (1:200; Novus, 19532) with 3% normal goat serum. Then, the sections were washed 5× for 10 minutes in PBST and soaked in 5% normal goat serum in PBST containing corresponding secondary antibodies, goat antimouse IgG-Alexa 488 (green; 1:500; Invitrogen), for 90 minutes. Finally, sections were washed 5× for 10 minutes in PBST and 3× for 5 minutes in PBS, processed for Hoechst 33258 (bisBenzimideH 33258 trihydrochloride, Sigma) for 30 minutes, washed in PBS, and cover-slipped with Fluoromount (Sigma). Spleen sections were examined using a confocal microscope (Olympus). Control studies included exclusion of primary antibody substituted with 5% normal goat serum in PBS. No immunoreactivity was observed in these controls.

Morphometric Analysis of TNF-α Positive Cells in the Spleen

Using sets of 1 of 6 sections, ≈4 systematically random sections of spleen tissue per animal, the density of TNF-α positive cells was measured. A rectangular contour was used, and the location of random plots within the red pulp of the spleen was determined by a counting sample frame of 250 μm×50 μm[32,33] to minimize bias. A total of 6 counting plots were generated randomly covering the rectangular area per section, and the number of TNF-α positive cells per unit area (density) was quantified throughout the spleen.[32,33]

Human Nuclei (HuNu) Staining

Every 1 of 6 40-mm-thick coronal tissue sections of brain and 20-mm-thick sections of spleen tissue, spanning the area of injury in the case of the brain and the entire red pulp in the case of spleen were randomly selected for quantitative analysis. Free floating sections were washed 3× for 5 minutes in PBS. For HuNu staining, samples were blocked for 60 minutes at room temperature with 5% normal goat serum (Invitrogen, CA) in PBS containing 0.1% Tween 20 (PBST; Sigma). Sections were then incubated overnight at 4°C with mouse monoclonal anti-HuNu (1:50; Millipore, MAB1281) with 5% normal goat serum. The sections were washed 5× for 10 minutes in PBST and then soaked in 5% normal goat serum in PBST containing corresponding secondary antibodies, goat antimouse IgG-Alexa 488 (green; 1:500; Invitrogen), for 90 minutes. Finally, sections were washed 5× for 10 minutes in PBST and 3× for 5 minutes in PBS, then processed for Hoechst 33258 (bisBenzimideH 33258 trihydrochloride, Sigma) for 30 minutes, washed in PBS, and cover-slipped with Fluoromount (Sigma). Brain and spleen sections were examined using a confocal microscope (Olympus). Control studies included exclusion of primary antibody substituted with 5% normal goat serum in PBS. No immunoreactivity was observed in these controls.

Stereological Analysis

Unbiased stereology was performed on brain sections immunostained with MHCII (OX6 staining). Sets of 1 of 6 sections, ≈8 systematically random sections, of about 240 μm apart, were taken from the brain spanning AP +2.00 mm to AP −4.56 mm in all 15 rats. Of note, section thicknesses were confirmed as being between 20.0 and 1.0 μm after dehydration, and this did not statistically differ between groups. MHCII positive cells were examined using the Cavalieri estimator probe of the unbiased stereological cell technique[34] revealing the volume of MHCII+ in gray and white matter areas, including striatum, subventricular zone, hilus, corpus callosum, internal capsule, and hippocampal fornix in both hemispheres (ipsilateral and contralateral). All samplings were optimized to count at least 300 cells per animal

with error coefficients <0.07. The Cavalieri estimator was executed using a point grid spaced equally both across and down directions. A grid space of 100 µm was used to cover the different gray and white matter regions each one representing our region of interest.[34]

Statistical Analysis

All data were expressed as mean±SEM and statistically evaluated using 1-way or 2-way ANOVA followed by Bonferonni's test (GraphPad version 5.01). In addition, Student *t* tests were also used to determine and compare the effect of hBMSC-transplanted stroke animals versus vehicle-infused stroke animals on TNF-α expression in the spleen. All comparisons were considered significant at $P<0.05$.

Results

Preferential Migration of hBMSCs to Spleen

ANOVA revealed that there was a significant treatment effects based on fluorescent signals detected in the spleen ($F_{3,11}=4.953$, $P<0.001$; Figure 1A and 1B). Pairwise comparison using post hoc tests revealed that hBMSC-DiR+ transplanted cells migrated to the spleen, emitting significantly higher fluorescent signals across all time points compared with hBMSC-DiR− transplanted and vehicle-infused stroke animals, and sham animals ($P<0.05$). Moreover, within the hBMSC-DiR+ transplanted stroke group, there were no significant differences in fluorescent signals across all time points except the first hour, whereby a higher emitted signal was found within spleen and on day 11 where the signal was greatly reduced relative to other time points ($P<0.05$). The signal that we detected from the transplanted group was specific for the DiR labeling because hBMSC-DiR− transplanted and vehicle-infused stroke animals, and sham animals, which were similarly subjected to the imaging assay displayed no detectable fluorescent signal (Figure 1A and 1B).

Similarly, ANOVA revealed significant treatment effects on brain migration as detected by fluorescent signals ($F_{3,11}=8.788$, $P<0.05$; Figure 1C and 1D). Pairwise comparisons using post hoc tests revealed that hBMSC-DiR+ cells migrated to the head area and emitted significantly higher fluorescent signals across all time points compared with hBMSC-DiR− transplanted and and vehicle-infused stroke animals, and sham animals ($P<0.05$). Within the hBMSC-DiR+ transplanted stroke animals, the fluorescent signals detected at 12 hours and 11 days were significantly higher than other time points ($P<0.05$). Comparing the spleen and the brain fluorescent signals within the hBMSC-DiR+ transplanted stroke animals showed that the splenic signals were significantly higher than those signals from the head area ($P<0.05$; Figure 1A and 1C). There were no fluorescent signals detected in the head region of hBMSC-DiR− transplanted and vehicle-infused stroke animals, and sham animals.

Harvested Organs Confirm Preferential hBMSC Migration to Spleen

ANOVA revealed that there was a significant treatment effect based on fluorescent signals detected in peripheral organs and

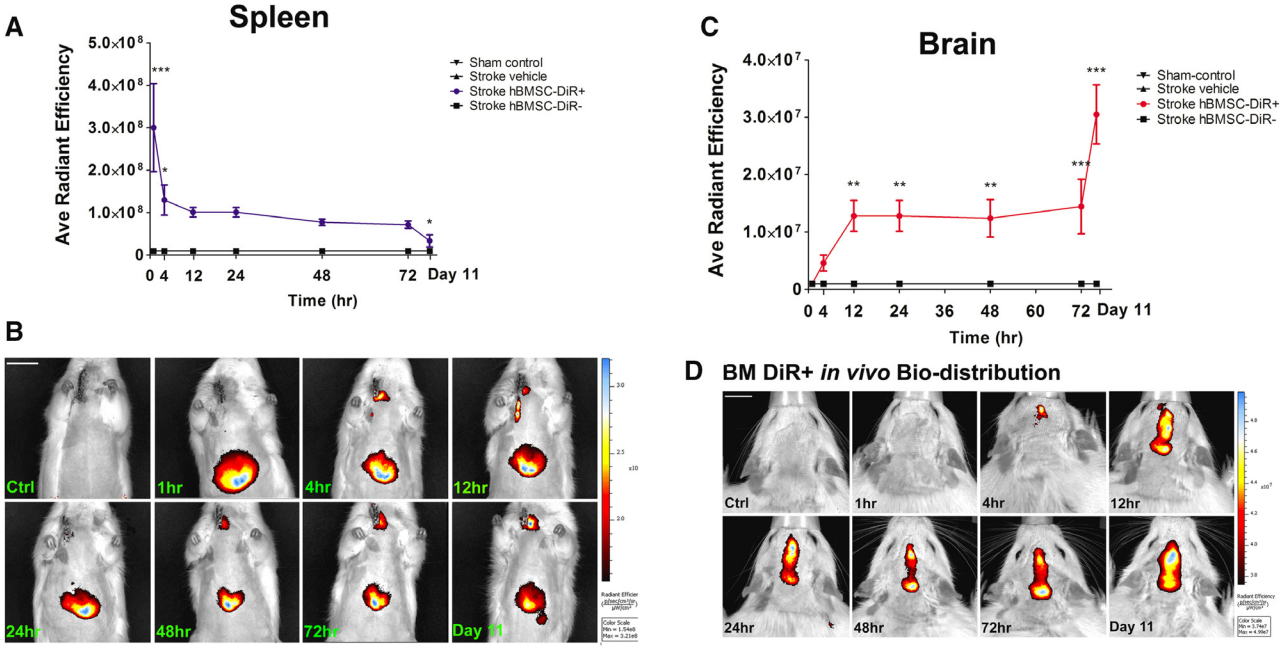

Figure 1. Preferential in vivo migration of hBMSC-DiR+ to spleen in chronic stroke. Representative images of in vivo fluorescence imaging of intravenously transplanted hBMSCs in an experimental model of chronic stroke at 1, 4, 12, 24, 48, and 72 hours and 11 days post transplantation. Photographs were taken from ventral (body) and dorsal positions (head). Imaging analyses revealed that hBMSC-DiR+ cells displayed a preferential migration to the spleen over the brain when transplanted at 60 days post stroke (***$P<0.001$). **A** and **B**, Within the hBMSC-DiR+ transplanted stroke group, there were no significant differences in fluorescent signals across all time points except the first hour, whereby a higher emitted signal was found within spleen and on day 11 where the signal was greatly reduced relative to other time points (*$P<0.05$). **C** and **D**, Fluorescent signals were also elevated in the head area at 12 hours and 11 days post transplantation (**$P<0.01$ and ***$P<0.001$). There were no fluorescent signals detected in the spleen and head region of hBMSC-DiR− transplanted and vehicle-infused stroke animals, and sham animals. Radiant efficiency={(p/s/cm^2/sr)/(µW/cm^2)}, color scale: min=1.54×10^8; max=3.2×10^8. *$P<0.05$, **$P<0.01$, and ***$P<0.001$. Data are expressed as mean±SEM. DiR indicates 1,1′-dioctadecyl-3,3,3′,3′-tetramethylindotricbocyanine iodide; and hBMSC, homing and anti-inflammatory effects of bone marrow stromal cells.

brain ex vivo ($F_{3,11}$=15.25, P<0.001; Figure 2A–2C). Pairwise comparisons using post hoc tests revealed that the brain emitted a significantly lower fluorescent signal relative to the spleen of rats exposed to chronic stroke (P<0.05). The liver and lung also emitted significantly higher signals than the brain, but the spleen displayed the most prominent fluorescent signals among the peripheral organs (P<0.05).

hBMSCs Reduce Striatal Infarct and Peri-Infarct Area, But Not Hippocampal Cell Loss

ANOVA revealed significant treatment effects on infarct area ($F_{2,12}$=25.66, P<0.001) and peri-infarct area ($F_{2,12}$=23.27, P<0.001; Figure 3A and 3B). Post hoc test revealed significant infarct and peri-infarct area in the ipsilateral (P<0.001), but not the contralateral (P>0.05) striatum of vehicle-infused stroke animals compared with sham animals In addition, there were significant infarct and peri-infarct areas in the ipsilateral (P<0.001), but not the contralateral (P>0.05) striatum of hBMSC-transplanted animals relative to sham animals (P<0.001). Interestingly, there were significant reductions of 15% and 30% in infarct and peri-infarct in the ipsilateral striatum, respectively, of hBMSC-transplanted stroke animals relative to vehicle-infused stroke animals (P<0.05; Figure 3A and 3B). There were no significant differences between the contralateral striatum of hBMSC-transplanted stroke animals and vehicle-infused stroke animals.

ANOVA revealed significant treatment effects in hippocampal CA1 neurons ($F_{2,12}$=5.15, P<0.001) and CA3 neurons (CA3, $F_{2,12}$=8.76, P<0.001). Post hoc test revealed significant neuronal cell loss in the ipsilateral (P<0.01), but not the contralateral hippocampal CA1 and CA3 area of vehicle-infused stroke animals compared with sham animals (P>0.05). In addition, there was significant neuronal cell loss in the ipsilateral (P<0.01), but not contralateral (P>0.05) CA1 and CA3 in hBMSC-transplanted stroke animals compared with sham animals. However, there was no significant reduction in CA1 and CA3 neuronal cell loss in rats that received hBMSCs-transplanted stroke animals compared with vehicle-infused stroke animals (P>0.05; Figure 3C and 3D). There were no significant differences in contralateral CA1 and CA3 neuronal cell loss between hBMSC-transplanted stroke animals and vehicle-infused stroke animals (P>0.05).

hBMSCs Ameliorate Stroke-Induced Neuroinflammation

The estimated volume of MHCII+ activated cells was quantified using stereological techniques. Several brain regions were examined to reveal stroke-induced neuroinflammation in both gray and white matter areas (Figure 4A and 4B). ANOVA revealed overall significant treatment effect on inflammation in the subcortical regions as evidenced by MHCII immunostaining in all gray matter regions examined here as follows: striatum ($F_{5,24}$=10.13, P<0.0001); subventricular zone ($F_{5,24}$=140.7, P<0.0001); and hilus ($F_{5,24}$=16.51, P<0.0001). Post hoc test revealed significant upregulation of activated MHCII+ cells in the ipsilateral side of vehicle-infused stroke animals compared with their contralateral side across all gray matter areas analyzed (P<0.0001), except subventricular zone (P>0.05). There were significant upregulation of activated MHCII+ cells in both ipsilateral and contralateral gray matter

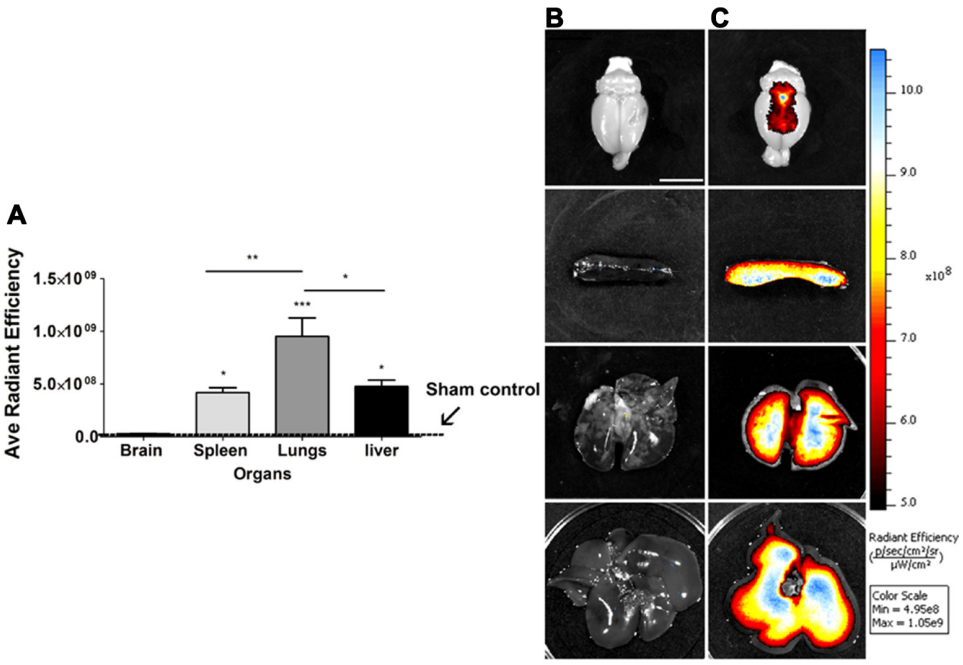

Figure 2. Preferential ex vivo migration of hBMSC-DiR+ to spleen in chronic stroke. **A**, Quantitative analysis of fluorescent signals brain, spleen, lungs, and liver confirmed preferential migration of hBMSC-DiR+ to the spleen over the brain (*****P<0.05). **B**, Photographs correspond to representative peripheral organs ex vivo. **B**, Sham animals (brain, spleen, lungs, and liver) and (**C**) hBMSC-DiR+ (brain, spleen, lungs, and liver). Radiant efficiency={(p/sec/cm2/sr)/(μW/cm2)}, color scale: min=3.74×10^7; max=4.99×10^7. *P<0.05, **P<0.01, and ***P<0.001. Data are expressed as mean±SEM. DiR indicates 1,1′-dioctadecyl-3,3,3′,3′-tetramethylindotricbocyanine iodide; and hBMSC, homing and anti-inflammatory effects of bone marrow stromal cells.

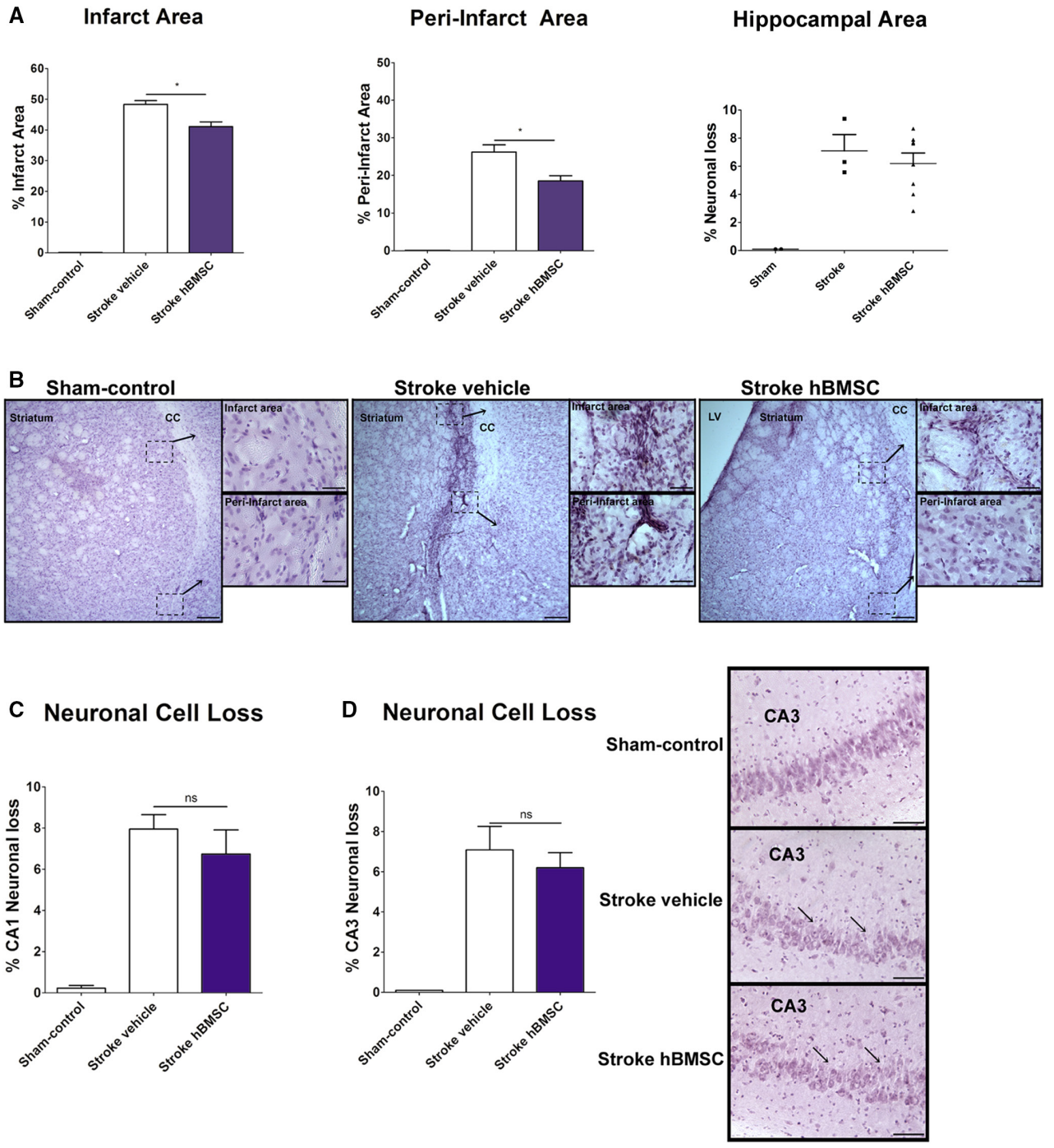

Figure 3. Homing and anti-inflammatory effects of bone marrow stromal cells (hBMSC) transplantation reduces infarct and peri-infarct area, but does not ameliorate hippocampal CA1 and CA3 neuronal loss. Hematoxylin and eosin (H&E) staining revealed that hBMSC treatment significantly reduced the striatal infarct and peri-infarct areas associated with stroke. **A**, Quantitative analysis revealed a significant reductions in infarct and peri-infarct area after hBMSC transplantation compared with vehicle-infused stroke animals (*P<0.05). **B**, Photomicrographs are representative coronal brain sections stained with H&E at 11 days post transplantation, showing infarct area (dark purple) and intact areas (light purple). Arrows denote infarct and peri-infarct area of striatum. Right inserts, vehicle-infused stroke exhibited acidic cells (dark purple cells), shrinkage, and dissolution of the cells in the infarcted striatum and peri-infarct area compared with the corresponding ipsilateral side of hBMSC-transplanted stroke animals. Scale bar: 1 mm. **C** and **D**, Quantitative analyses of total number of CA1 and CA3 neurons failed to reveal a significant reduction in neuronal cell loss in rats that received hBMSCs compared with vehicle-infused stroke rats (*P>0.05). **C** and **D**, Photomicrographs are representative coronal brain sections staining with H&E from ipsilateral CA1 and CA3 area of the hippocampus of sham, vehicle-infused, and hBMSC-treated stroke animals. Arrows denote neuronal cell loss within the CA1 and CA3 region. Scale bar=50 μm. *P<0.05; ns=not significant. Data are expressed as percentage difference from contralateral CA1 and CA3 total number of neurons.

areas of vehicle-infused stroke animals compared with sham animals (P<0.0001). There were also significant upregulation of activated MHCII+ cells in both ipsilateral and contralateral side of hBMSC-transplanted stroke animals across all gray matter areas analyzed compared with sham animals (P<0.05; Figure 4A and 4B). There were significant reductions in

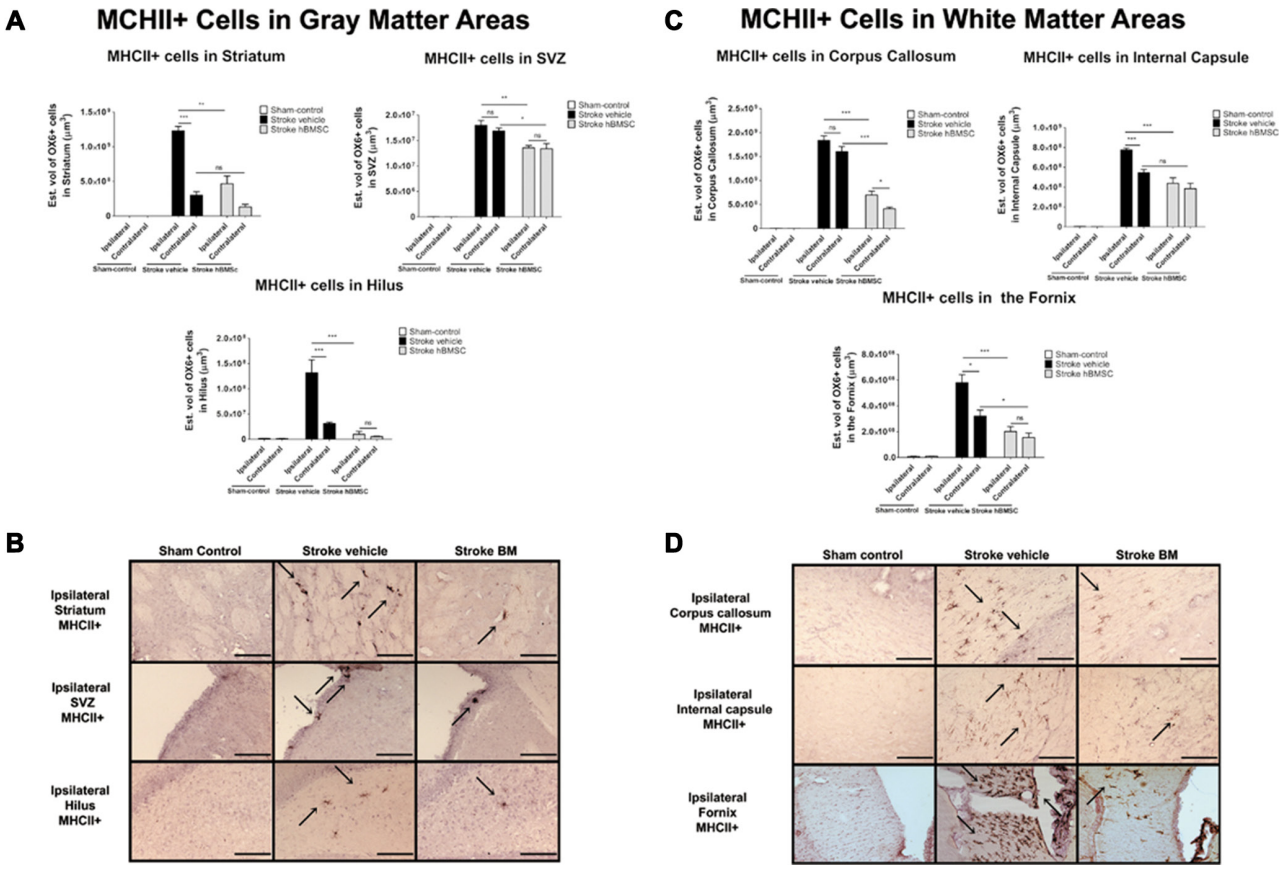

Figure 4. Homing and anti-inflammatory effects of bone marrow stromal cells (hBMSC) transplantation ameliorates neuroinflammation in gray and white matter areas in chronic stroke. **A**, Stereological analysis of MHCII+ cells estimated volume in striatum, subventricular zone (SVZ), and hilus revealed significant upregulation of activated MHCII+ cells in the ipsilateral side of vehicle-infused stroke animals compared with their contralateral side across all gray matter areas analyzed (***P<0.0001), except SVZ (P>0.05). There were significant upregulation of activated MHCII+ cells in both ipsilateral and contralateral gray matter areas of vehicle-infused stroke animals (P<0.0001) and hBMSC-transplanted stroke animals compared with sham animals (P<0.05). hBMSC transplantation caused a 35%, 28%, and 90% reduction of the estimated volume of MHC+ cells in the ipsilateral striatum, SVZ, and hilus, respectively, relative to the ipsilateral side of the same regions of vehicle-infused stroke animals (**P<0.01; **P<0.01; ***P<0.001). **B**, Photomicrographs are representative coronal brain sections ipsilateral to injury stained with MHCII 11 days post hBMSC transplantation. Arrows indicate positive staining for activated MHCII+ cells in striatum, SVZ, and hilus. **C**, Effects of hBMSC transplantation on MHCII+ cells in white matter regions. Stereological analysis of MHCII+ cells estimated volume in corpus callosum, internal capsule, and fornix revealed significant upregulation of activated MHCII+ cells in the ipsilateral side of vehicle-infused stroke animals compared with their contralateral side across all white matter areas analyzed (***P<0.0001), except corpus callosum (P>0.05). There were significant upregulation of activated MHCII+ cells in both ipsilateral and contralateral side of vehicle-infused stroke animals (***P<0.0001) and hBMSC-transplanted stroke animals across all white matter areas analyzed compared with sham animals (*P<0.05). hBMSC transplantation caused a 60%, 38%, and 70% reduction of the estimated volume of MHCII+ cells in the ipsilateral corpus callosum, internal capsule, and fornix, respectively, relative to the ipsilateral side of the same regions of vehicle-infused stroke animals (***P<0.001). **D**, Photomicrographs are representative coronal brain sections ipsilateral to injury stained with MHCII 11 days post hBMSC transplantation. Arrows indicate positive staining for activated MHCII+ cells. Scale bar=50 μm. *P<0.05, **P<0.01, and ***P<0.001; ns=not significant. Data are expressed as mean±SEM. MHCII indicates major histocompatibility complex II.

activated MHCII+ cells in both ipsilateral and contralateral side of hBMSC-transplanted stroke animals across all gray matter areas analyzed compared with the ipsilateral and contralateral side of vehicle-infused stroke animals (P<0.001), indicating efficacy of the treatment. Moreover, the reduction of activated MHCII+ cells in the ipsilateral side of hBMSC-transplanted stroke animals did not significantly differ to their contralateral side across all gray matter areas analyzed (P>0.05).

Similarly, ANOVA demonstrated significant treatment effects on inflammation in several white matter subcortical regions as evidenced by MHCII+ immunostaining in all regions examined here as follows: corpus callosum ($F_{5,24}$=188.9, P<0.0001), internal capsule ($F_{5,24}$=43.30, P<0.0001), and fornix ($F_{5,24}$=35.70, P<0.0001; Figure 4C and 4D). Post hoc test revealed significant upregulation of activated MHCII+ cells in the ipsilateral side of vehicle-infused stroke animals compared with their contralateral side across all white matter areas analyzed (P<0.0001), except corpus callosum (P>0.05). There were significant upregulation of activated MHCII+ cells in both ipsilateral and contralateral side of vehicle-infused stroke animals across all white matter areas analyzed compared with sham animals (P<0.0001). There were significant upregulation of activated MHCII+ cells in both ipsilateral and contralateral side of hBMSC-transplanted stroke animals across all white matter areas analyzed compared with sham animals

(P<0.05). There was also a significant upregulation of activated MHCII+ cells in the ipsilateral side of hBMSC-transplanted stroke animals compared with their contralateral side across all white matter areas analyzed (P<0.05), except corpus callosum (P>0.05). There were significant reductions of activated MHCII+ cells in the ipsilateral side of hBMSC-transplanted stroke animals across all white matter areas analyzed compared with the ipsilateral side of vehicle-infused stroke animals (P<0.001), indicating efficacy of the treatment similar to that observed in gray matter areas. In addition, there were significant reductions of activated MHCII+ cells in the contralateral side of hBMSC-transplanted stroke animals across all white matter areas analyzed compared with the contralateral side of vehicle-infused stroke animals (P<0.001), except in the internal capsule (P>0.05; Figure 4C and 4D).

hBMSCs Survive Better in the Spleen Than the Brain

Confocal microscopy of hBMSC survival using immunofluorescent demonstrated positive expression in spleen and brain of hBMSC-transplanted stroke animals (Figure 5A). HuNu positive cells were found in the spleen and brain (Figure 5A). The mean graft survival of hBMSCs (ie, HuNu expression) in the spleen was significantly higher than that found in the brain indicating preferential hBMSC migration to the spleen (Student t test, P<0.05). An estimated 0.03% of hBMSCs survived in the spleen compared with 0.0007% survival in the brain (Figure 5B and 5C).

hBMSCs Diminish TNF-α Density in Spleen

TNF-α expression in the spleen was analyzed using immunofluorescence to reveal anti-inflammatory effects of hBMSCs on splenic function. The mean TNF-α density in the spleen was highly elevated in vehicle-infused stroke animals which was significantly downregulated by hBMSC transplantation (Student t test, P<0.05; Figure 6A and 6B).

Correlation Between hBMSC Migration to Spleen and Stroke Functional Outcomes

Recognizing that the spleen was preferentially targeted by hBMSCs, we conducted correlational analyses to reveal whether this splenic migration of hBMSCs correlated with the observed functional outcomes. Pearson's correlation analysis revealed negative correlations between hBMSC migration in the spleen and the infarct and peri-infarct areas (infarct area: Pearson r=–0.8678, R^2=–0.7531, P<0.01; peri-infarct area: Pearson r=–0.8282, R^2=–0.6859, P<0.02; Figure 6C, top panel). Furthermore, correlational analysis revealed a negative correlation between hBMSC migration in the spleen and the volume of MHCII+ activated cells in the striatum (Pearson r=–0.8656, R^2=–0.7492, P<0.02; Figure 6C, bottom panel left). In addition, a negative correlation was detected between hBMSC migration in the spleen and the density of TNF-α expression in the spleen (Pearson r=–0.8381, R^2=–0.7025, P<0.03; Figure 6C bottom panel right).

Discussion

The study demonstrated preferential migration of intravenously delivered hBMSCs to the spleen over the brain in adult rats with chronic stroke as evidenced by in vivo and ex vivo imaging analyses. Transplantation of hBMSCs reduced the infarct and peri-infarct area in the striatum, but failed to

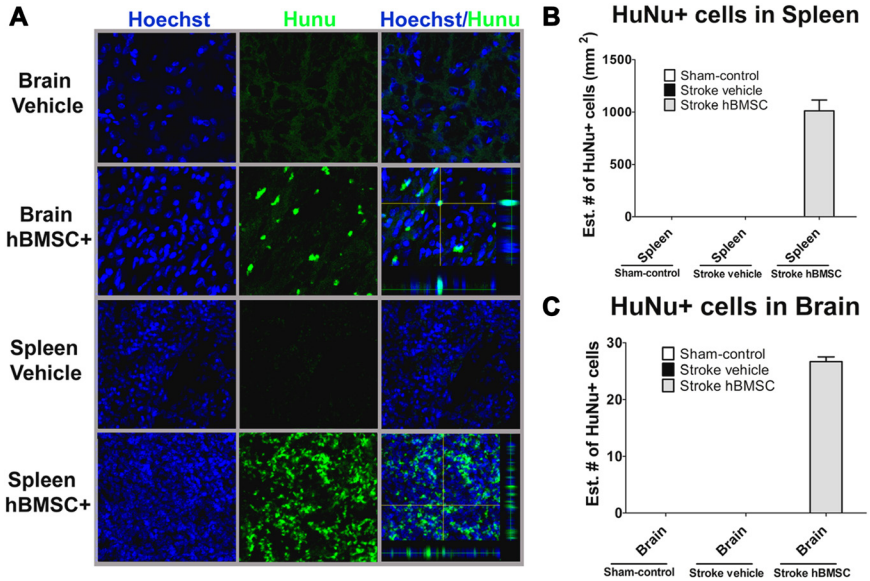

Figure 5. Homing and anti-inflammatory effects of bone marrow stromal cells (hBMSCs) survive better in the spleen than the brain. **A**, Representative merged images showing colocalization of HuNu+ and Hoeschst+ expression from grafted hBMSCs in spleen and brain (ie, striatum) in transplanted stroke rats as opposed to vehicle-infused stroke rats. **Top right**, Z-stack reconstruction of HuNu+ hBMSCs (green, human-specific antigen) within the spleen colocalized with Hoechst+ (blue, nuclei marker) in hBMSC-transplanted stroke animals. **Bottom right**, Z-stack reconstruction of HuNu+ hBMSCs (green) within the peri-infarct area of the striatum colocalized with Hoechst+ (blue) in hBMSC-transplanted stroke animals. Quantitative analyses of the estimated number of HuNu+ hBMSCs in the spleen (**B**) and in the brain (**C**) of hBMSC-transplanted stroke animals revealed 0.03% of hBMSCs survived in the spleen compared with 0.0007% survival in the brain, indicating that the mean graft survival, and likely preferential migration, of hBMSCs in the spleen was significantly higher than that found in the brain. Scale bar=50 μm. Data are expressed as mean±SEM.

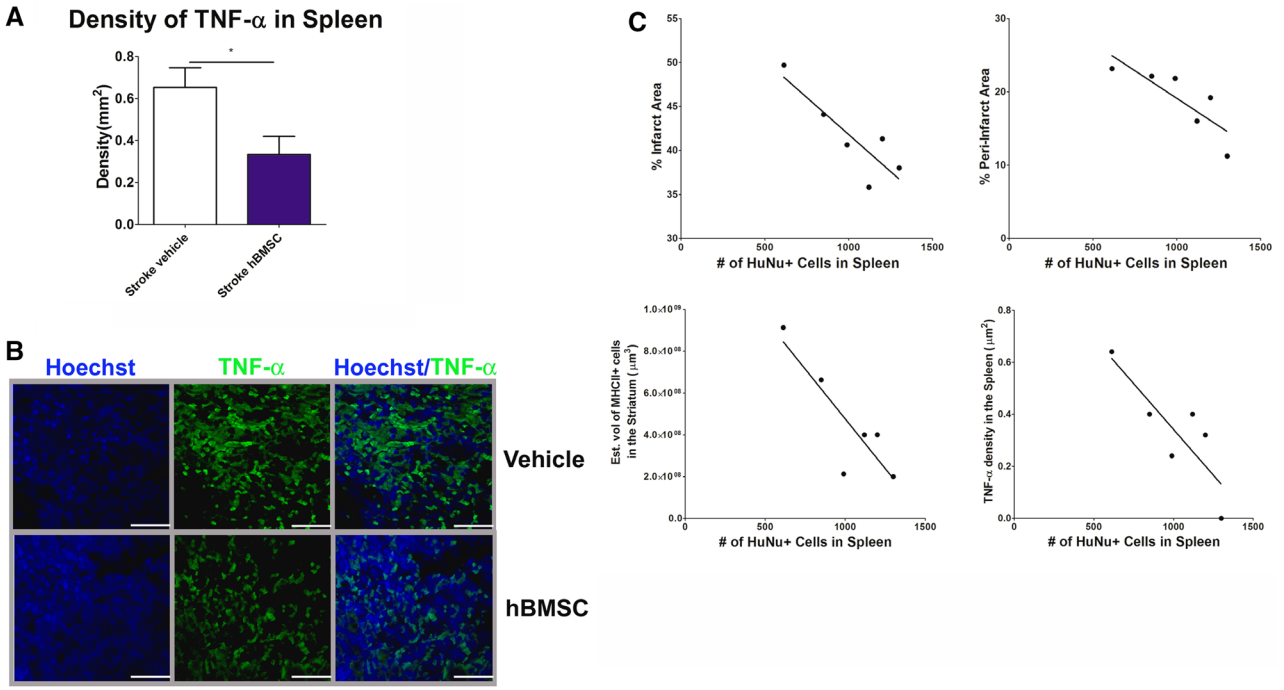

Figure 6. Homing and anti-inflammatory effects of bone marrow stromal cells (hBMSCs) reduced tumor necrosis factor-α (TNF-α) density in the spleen of stroke animals. **A**, Quantitative analysis of TNF-α expression in the spleen revealed a significant upregulation of TNF-α density in vehicle-infused stroke animals. In contrast, hBMSC treatment promoted a 40% downregulation of TNF-α density in the spleen (**P*<0.05). **B**, Confocal photomicrographs of positive expression of TNF-α (green) and Hoechst (blue) in the spleen of vehicle-infused (**top**) and transplanted stroke animals (**bottom**), indicating decreased expression of TNF-α in the spleen of hBMSC-transplanted stroke animals relative to vehicle-infused stroke animals. **C**, Correlations found between reduction in striatal infarct and peri-infarct areas, downregulation of MHCII+ cells in brain, and decreased density of TNF-α in the spleen, and the number of hBMSCs that migrated to the spleen (% infarct area: Pearson *r*=–0.8678, R^2=–0.7531, *P*<0.01; % peri-infarct area: Pearson *r*=–0.8282, R^2=–0.6859, *P*<0.05; the volume of MHCII+ activated cells in the striatum: Pearson *r*=–0.8656, R^2=–0.7492, *P*<0.05; the density of TNF-α expression in the spleen: Pearson *r*=–0.8381, R^2=–0.7025, *P*<0.05). Scale bar=50 μm. **P*<0.05. Data are expressed as mean±SEM.

ameliorate the hippocampal CA1 and CA3 neuronal cell loss. In addition, hBMSCs attenuated stroke-induced inflammation in subcortical gray and white matter regions in the brain coupled with downregulation of TNF-α density in the spleen. Moreover, it was observed that hBMSCs survived better in the spleen than the brain, which correlated with amelioration of neurostructural deficits and inflammation. Together, these findings support our hypothesis of hBMSC preferential migration to the spleen in affording therapeutic benefits against chronic stroke possibly by targeting the ongoing secondary neurodegeneration largely mediated by splenic inflammation.

Preferential migration, toward the site of pathological signals, plays a key role in realizing the therapeutic benefits of stem cell transplantation. As proof of this concept, preclinical data indicate that after stroke injury endogenous and exogenously transplanted BMSCs migrate to the spleen through a chemoattractant signaling pathway.[35] Such deposition of systemically delivered stem cells into the spleen after stroke is accompanied by reduced necrotic and apoptotic cell death in the brain, decreased motor and cognitive deficits, and dampened splenic inflammatory response.[25,36–39] This sequestration of neurodegeneration by suppressing systemic inflammation originating from the spleen was previously demonstrated in stroke animals that had their spleen removed or transplanted with human umbilical cord cells in the acute stage of stroke.[25,36] The present in vivo imaging revealed hBMSC deposition to the spleen in the chronic stage of stroke, supporting the notion that attenuating the splenic inflammatory response offers a novel strategy and a wider therapeutic window for treating stroke.

Infarct and peri-infarct areas and hippocampal neuronal degeneration are hallmark of the cessation of blood flow after ischemic stroke characterized by massive neuronal cell death and progressive secondary neurodegeneration.[9,10,27,36] Our group along, with others, have demonstrated that transplantation of adult stem cells afford extensive therapeutic benefits, including decreased neuronal cell death and reduction of infarct and peri-infarct volumes and hippocampal cell loss.[7,40,41] Our present data showed, although still impaired compared with sham animals, that intravenous transplantation of hBMSC, at 60 days post stroke, exerted reduced striatal infarct and peri-infarct area. There was only a trend toward reduction in hippocampal CA1 and CA3 cell loss, likely because of the susceptibility of these hippocampal cells to neuroinflammation and excitotoxicity during chronic ischemic insults,[42] which reduces the likelihood of regeneration.[42,43] Conversely, striatal cholinergic interneurons compared with hippocampal CA1 and CA3 interneurons tend to be less vulnerable to chronic ischemic insults,[44,45] and therefore may be more amenable to regeneration. These findings are in line with previous reports in which reduced striatal infarcts and only partial recovery of hippocampal-dependent neurological functions were achieved post BMSC transplantation.[43,46,47]

Activated monocytes, macrophages, and microglia cells in the area of injury could contribute to ischemic injury via synaptic damage, phagocytosis, and through the release of cytotoxins after stroke.[48–50] Cytotoxins induce chronic activation and exacerbation of microglia and antigen-presenting cells (MHCII+) instigating further upregulation of inflammatory mediators, such as tumor necrosis factor-α (TNF-α), IL-1β, nitric oxide, and reactive oxygen species causing edema, necrosis, and apoptosis.[51,52] Interestingly, the levels of TNF-α and other cytokines, such as IL-1 and IL-6, in the cerebrospinal fluid and plasma have been implicated as key inflammatory molecules associated with the extent of ischemic stroke in both animal models and human patients.[53–55] Accordingly, these cytokines may be targeted for therapeutic purposes, but may equally serve as potent biomarkers for stroke. In this study, a massive chronic neuroinflammation was evident in both ipsilateral and contralateral gray and white matter areas of vehicle-infused stroke animals relative to sham animals, which was reduced by hBMSC transplantation. BMSCs possessed the capacity to switch antigen-presenting cells from MHCII+ inflammatory cells to anti-inflammatory cell phenotype in different disease models, including ischemic and inflammatory lung disease.[56–61] These results not only imply immune-modulation and anti-inflammatory benefits by systemic transplantation of hBMSCs, but support the concept of the bystander effect. Moreover, instead of cell engraftment at the area of injury,[62,63] hBMSC migration to the spleen, where the grafts seem to exert their maximal anti-inflammation effects, likely mediated the observed therapeutic benefits.

To date, preclinical studies reporting functional outcomes of systemic delivery of stem cells in stroke models favor transplantation during acute stroke (ie, 1 hour to 3 days post stroke transplantation), and only 1 laboratory study (1 month after stroke induction surgery) and 1 preclinical trial (transplantation at 23–37 days after stroke onset) have shown efficacy of peripheral transplantation at the chronic stage of stroke.[64,65] Moreover, even when systemic transplantation targets the acute stroke allowing cell deposition into peripheral organs, there was neither behavioral recovery nor neuroprotection observed.[66–68] Nevertheless, comparing the results of the current study to those of the previous reports is somewhat difficult given the differences in experimental procedures, such as BMSC dosage, timing, and route of administration, and animal species used. More importantly, an emphasis on evaluating the successful migration of BMSCs to the spleen and the resulting splenic inflammatory responses may provide key insights into the functional outcomes of systemic BMSC transplant studies.

This study supports an alternative mechanism underlying cell therapy for stroke, advancing the notion that the entry of stem cells into the brain may not be a prerequisite in producing functional recovery. That transplanted MSCs were scarcely detected in the brain, but instead preferentially migrated to the spleen suggests that sequestration of splenic peripheral inflammation may be the primary mode of action of grafted stem cells. Indeed, many of neural transplantation studies fail to detect good graft survival and persistence in the brain, despite robust functional recovery of stroke animals. Our present study resolves this perplexing gap in the central nervous system cell therapy literature in that in the absence of robust graft survival in the brain, preferential homing of stem cells to the spleen and thereupon affording anti-inflammatory may mitigate stroke symptoms.

In summary, we demonstrated here that preferential migration of the BMSCs to the spleen is an effective approach in dampening the inflammation-plagued secondary cell death associated with chronic stroke. Enhancing the bioavailability of systemically transplanted BMSCs or their secreted factors, especially the anti-inflammatory molecules, in the spleen during the stroke progression warrants further investigation.

Sources of Funding

This research was funded by the National Institute of Neurological Disorders and Stroke 1R01NS071956-01A1, 1R21NS089851-01, and James and Esther King Biomedical Research Foundation 1KG01-33966.

Disclosures

Dr Borlongan has patents and patent applications on stem cell therapy. The other authors report no conflicts.

References

1. Adamson J, Beswick A, Ebrahim S. Is stroke the most common cause of disability? *J Stroke Cerebrovasc Dis*. 2004;13:171–177. doi: 10.1016/j.jstrokecerebrovasdis.2004.06.003.
2. Go AS, Mozaffarian D, Roger VL, Benjamin EJ, Berry JD, Borden WB, et al. Heart disease and stroke statistics-2013 update: a report from the American Heart Association. *Circulation*. 2013;127:6–245.
3. Lo EH, Dalkara T, Moskowitz MA. Mechanisms, challenges and opportunities in stroke. *Nat Rev Neurosci*. 2003;4:399–415. doi: 10.1038/nrn1106.
4. Hacke W, Kaste M, Bluhmki E, Brozman M, Dávalos A, Guidetti D, et al; ECASS Investigators. Thrombolysis with alteplase 3 to 4.5 hours after acute ischemic stroke. *N Engl J Med*. 2008;359:1317–1329. doi: 10.1056/NEJMoa0804656.
5. The NINDS rt-PA Stroke Study Group. Intracerebral hemorrhage after intravenous tPA therapy for ischemic stroke. *Stroke*. 1997;28:2109–2118.
6. Wang X, Tsuji K, Lee SR, Ning M, Furie KL, Buchan AM, et al. Mechanisms of hemorrhagic transformation after tissue plasminogen activator reperfusion therapy for ischemic stroke. *Stroke*. 2004;35(11 Suppl 1):2726–2730. doi: 10.1161/01.STR.0000143219.16695.af.
7. Tajiri N, Acosta S, Glover LE, Bickford PC, Jacotte Simancas A, Yasuhara T, et al. Intravenous grafts of amniotic fluid-derived stem cells induce endogenous cell proliferation and attenuate behavioral deficits in ischemic stroke rats. *PLoS One*. 2012;7:e43779. doi: 10.1371/journal.pone.0043779.
8. Garbuzova-Davis S, Rodrigues MC, Hernandez-Ontiveros DG, Tajiri N, Frisina-Deyo A, Boffeli SM, et al. Blood-brain barrier alterations provide evidence of subacute diaschisis in an ischemic stroke rat model. *PLoS One*. 2013;8:e63553. doi: 10.1371/journal.pone.0063553.
9. Borlongan CV, Kaneko Y, Maki M, Yu SJ, Ali M, Allickson JG, et al. Menstrual blood cells display stem cell-like phenotypic markers and exert neuroprotection following transplantation in experimental stroke. *Stem Cells Dev*. 2010;19:439–452. doi: 10.1089/scd.2009.0340.
10. Borlongan CV, Lind JG, Dillon-Carter O, Yu G, Hadman M, Cheng C, et al. Bone marrow grafts restore cerebral blood flow and blood brain barrier in stroke rats. *Brain Res*. 2004;1010:108–116. doi: 10.1016/j.brainres.2004.02.072.
11. Matsukawa N, Yasuhara T, Hara K, Xu L, Maki M, Yu G, et al. Therapeutic targets and limits of minocycline neuroprotection in experimental ischemic stroke. *BMC Neurosci*. 2009;10:126. doi: 10.1186/1471-2202-10-126.
12. Sanberg PR, Eve DJ, Cruz LE, Borlongan CV. Neurological disorders and the potential role for stem cells as a therapy. *Br Med Bull*. 2012;101:163–181. doi: 10.1093/bmb/lds001.

13. Sanberg PR, Eve DJ, Metcalf C, Borlongan CV. Advantages and challenges of alternative sources of adult-derived stem cells for brain repair in stroke. *Prog Brain Res*. 2012;201:99–117. doi: 10.1016/B978-0-444-59544-7.00006-8.
14. Sanberg PR, Eve DJ, Willing AE, Garbuzova-Davis S, Tan J, Sanberg CD, et al. The treatment of neurodegenerative disorders using umbilical cord blood and menstrual blood-derived stem cells. *Cell Transplant*. 2011;20:85–94. doi: 10.3727/096368910X532855.
15. Zhang L, Yi L, Chopp M, Kramer BC, Romanko M, Gosiewska A, et al. Intravenous administration of human umbilical tissue-derived cells improves neurological function in aged rats after embolic stroke. *Cell Transplant*. 2013;22:1569–1576. doi: 10.3727/096368912X658674.
16. Savitz SI, Misra V, Kasam M, Juneja H, Cox CS Jr, Alderman S, et al. Intravenous autologous bone marrow mononuclear cells for ischemic stroke. *Ann Neurol*. 2011;70:59–69. doi: 10.1002/ana.22458.
17. Prasad K, Sharma A, Garg A, Mohanty S, Bhatnagar S, Johri S, et al; InveST Study Group. Intravenous autologous bone marrow mononuclear stem cell therapy for ischemic stroke: a multicentric, randomized trial. *Stroke*. 2014;45:3618–3624. doi: 10.1161/STROKEAHA.114.007028.
18. Moniche F, Montaner J, Gonzalez-Marcos JR, Carmona M, Piñero P, Espigado I, et al. Intra-arterial bone marrow mononuclear cell transplantation correlates with GM-CSF, PDGF-BB, and MMP-2 serum levels in stroke patients: results from a clinical trial. *Cell Transplant*. 2014;23 Suppl 1:S57–S64. doi: 10.3727/096368914X684934.
19. Banerjee S, Bentley P, Hamady M, Marley S, Davis J, Shlebak A, et al. Intra-Arterial Immunoselected CD34+ stem cells for acute ischemic stroke. *Stem Cells Transl Med*. 2014;3:1322–1330. doi: 10.5966/sctm.2013-0178.
20. Acosta SA, Tajiri N, Shinozuka K, Ishikawa H, Grimmig B, Diamond DM, et al. Long-term upregulation of inflammation and suppression of cell proliferation in the brain of adult rats exposed to traumatic brain injury using the controlled cortical impact model. *PLoS One*. 2013;8:e53376. doi: 10.1371/journal.pone.0053376.
21. Jin R, Yang G, Li G. Inflammatory mechanisms in ischemic stroke: role of inflammatory cells. *J Leukoc Biol*. 2010;87:779–789. doi: 10.1189/jlb.1109766.
22. Yepes M, Brown SA, Moore EG, Smith EP, Lawrence DA, Winkles JA. A soluble Fn14-Fc decoy receptor reduces infarct volume in a murine model of cerebral ischemia. *Am J Pathol*. 2005;166:511–520. doi: 10.1016/S0002-9440(10)62273-0.
23. Padma Srivastava MV, Bhasin A, Bhatia R, Garg A, Gaikwad S, Prasad K, et al. Efficacy of minocycline in acute ischemic stroke: a single-blinded, placebo-controlled trial. *Neurol India*. 2012;60:23–28.
24. Loddick SA, Rothwell NJ. Neuroprotective effects of human recombinant interleukin-1 receptor antagonist in focal cerebral ischaemia in the rat. *J Cereb Blood Flow Metab*. 1996;16:932–940. doi: 10.1097/00004647-199609000-00017.
25. Vendrame M, Gemma C, Pennypacker KR, Bickford PC, Davis Sanberg C, Sanberg PR, et al. Cord blood rescues stroke-induced changes in splenocyte phenotype and function. *Exp Neurol*. 2006;199:191–200. doi: 10.1016/j.expneurol.2006.03.017.
26. Walker PA, Shah SK, Jimenez F, Gerber MH, Xue H, Cutrone R, et al. Intravenous multipotent adult progenitor cell therapy for traumatic brain injury: preserving the blood brain barrier via an interaction with splenocytes. *Exp Neurol*. 2010;225:341–352. doi: 10.1016/j.expneurol.2010.07.005.
27. Ishikawa H, Tajiri N, Shinozuka K, Vasconcellos J, Kaneko Y, Lee HJ, et al. Vasculogenesis in experimental stroke after human cerebral endothelial cell transplantation. *Stroke*. 2013;44:3473–3481. doi: 10.1161/STROKEAHA.113.001943.
28. Hayashi T, Kaneko Y, Yu S, Bae E, Stahl CE, Kawase T, et al. Quantitative analyses of matrix metalloproteinase activity after traumatic brain injury in adult rats. *Brain Res*. 2009;1280:172–177. doi: 10.1016/j.brainres.2009.05.040.
29. Yu SJ, Soncini M, Kaneko Y, Hess DC, Parolini O, Borlongan CV. Amnion: a potent graft source for cell therapy in stroke. *Cell Transplant*. 2009;18:111–118.
30. Glover LE, Tajiri N, Lau T, Kaneko Y, van Loveren H, Borlongan CV. Immediate, but not delayed, microsurgical skull reconstruction exacerbates brain damage in experimental traumatic brain injury model. *PLoS One*. 2012;7:e33646. doi: 10.1371/journal.pone.0033646.
31. Paxinos G, Watson C. *The Rat Brain in Stereotaxic Coordinates*. 5th ed. San Diego, CA: Academic Press; 2005:1–456.
32. Armstrong RA, Kotzbauer PT, Perlmutter JS, Campbell MC, Hurth KM, Schmidt RE, et al. A quantitative study of α-synuclein pathology in fifteen cases of dementia associated with Parkinson disease. *J Neural Transm*. 2014;121:171–181. doi: 10.1007/s00702-013-1084-z.
33. Armstrong RA. Quantifying the pathology of neurodegenerative disorders: quantitative measurements, sampling strategies and data analysis. *Histopathology*. 2003;42:521–529.
34. Mayhew TM. The new stereological methods for interpreting functional morphology from slices of cells and organs. *Exp Physiol*. 1991;76:639–665.
35. Murray KN, Buggey HF, Denes A, Allan SM. Systemic immune activation shapes stroke outcome. *Mol Cell Neurosci*. 2013;53:14–25. doi: 10.1016/j.mcn.2012.09.004.
36. Vendrame M, Cassady J, Newcomb J, Butler T, Pennypacker KR, Zigova T, et al. Infusion of human umbilical cord blood cells in a rat model of stroke dose-dependently rescues behavioral deficits and reduces infarct volume. *Stroke*. 2004;35:2390–2395. doi: 10.1161/01.STR.0000141681.06735.9b.
37. Barbosa da Fonseca LM, Gutfilen B, Rosado de Castro PH, Battistella V, Goldenberg RC, Kasai-Brunswick T, et al. Migration and homing of bone-marrow mononuclear cells in chronic ischemic stroke after intra-arterial injection. *Exp Neurol*. 2010;221:122–128.
38. Vasconcelos-dos-Santos A, Rosado-de-Castro PH, Lopes de Souza SA, da Costa Silva J, Ramos AB, Rodriguez de Freitas G, et al. Intravenous and intra-arterial administration of bone marrow mononuclear cells after focal cerebral ischemia: Is there a difference in biodistribution and efficacy? *Stem Cell Res*. 2012;9:1–8. doi: 10.1016/j.scr.2012.02.002.
39. Huang W, Mo X, Qin C, Zheng J, Liang Z, Zhang C. Transplantation of differentiated bone marrow stromal cells promotes motor functional recovery in rats with stroke. *Neurol Res*. 2013;35:320–328. doi: 10.1179/1743132812Y.0000000151.
40. Yasuhara T, Borlongan CV, Date I. Ex vivo gene therapy: transplantation of neurotrophic factor-secreting cells for cerebral ischemia. *Front Biosci*. 2006;11:760–775.
41. Yasuhara T, Hara K, Maki M, Mays RW, Deans RJ, Hess DC, et al. Intravenous grafts recapitulate the neurorestoration afforded by intracerebrally delivered multipotent adult progenitor cells in neonatal hypoxic-ischemic rats. *J Cereb Blood Flow Metab*. 2008;28:1804–1810. doi: 10.1038/jcbfm.2008.68.
42. Nikonenko AG, Radenovic L, Andjus PR, Skibo GG. Structural features of ischemic damage in the hippocampus. *Anat Rec (Hoboken)*. 2009;292:1914–1921. doi: 10.1002/ar.20969.
43. Li Y, Hua X, Hua F, Mao W, Wan L, Li S. Are bone marrow regenerative cells ideal seed cells for the treatment of cerebral ischemia? *Neural Regen Res*. 2013;8:1201–1209. doi: 10.3969/j.issn.1673-5374.2013.13.005.
44. Calabresi P, Centonze D, Pisani A, Bernardi G. Metabotropic glutamate receptors and cell-type-specific vulnerability in the striatum: implication for ischemia and Huntington's disease. *Exp Neurol*. 1999;158:97–108. doi: 10.1006/exnr.1999.7092.
45. Chesselet MF, Gonzales C, Lin CS, Polsky K, Jin BK. Ischemic damage in the striatum of adult gerbils: relative sparing of somatostatinergic and cholinergic interneurons contrasts with loss of efferent neurons. *Exp Neurol*. 1990;110:209–218.
46. Liu Z, Li Y, Zhang ZG, Cui X, Cui Y, Lu M, et al. Bone marrow stromal cells enhance inter- and intracortical axonal connections after ischemic stroke in adult rats. *J Cereb Blood Flow Metab*. 2010;30:1288–1295. doi: 10.1038/jcbfm.2010.8.
47. Chen J, Zhang ZG, Li Y, Wang L, Xu YX, Gautam SC, et al. Intravenous administration of human bone marrow stromal cells induces angiogenesis in the ischemic boundary zone after stroke in rats. *Circ Res*. 2003;92:692–699. doi: 10.1161/01.RES.0000063425.51108.8D.
48. Hernandez-Ontiveros DG, Tajiri N, Acosta S, Giunta B, Tan J, Borlongan CV. Microglia activation as a biomarker for traumatic brain injury. *Front Neurol*. 2013;4:30. doi: 10.3389/fneur.2013.00030.
49. Yin D, Yan X, Fan M, Hu Y, Men W, Sun L, et al. Secondary degeneration detected by combining voxel-based morphometry and tract-based spatial statistics in subcortical strokes with different outcomes in hand function. *AJNR Am J Neuroradiol*. 2013;34:1341–1347. doi: 10.3174/ajnr.A3410.
50. Delano-Wood L, Stricker NH, Sorg SF, Nation DA, Jak AJ, Woods SP, et al. Posterior cingulum white matter disruption and its associations with verbal memory and stroke risk in mild cognitive impairment. *J Alzheimers Dis*. 2012;29:589–603. doi: 10.3233/JAD-2012-102103.
51. Lucas SM, Rothwell NJ, Gibson RM. The role of inflammation in CNS injury and disease. *Br J Pharmacol*. 2006;147 Suppl 1:S232–S240. doi: 10.1038/sj.bjp.0706400.

52. Moro MA, Cárdenas A, Hurtado O, Leza JC, Lizasoain I. Role of nitric oxide after brain ischaemia. *Cell Calcium*. 2004;36:265–275. doi: 10.1016/j.ceca.2004.02.011.
53. Allan SM, Tyrrell PJ, Rothwell NJ. Interleukin-1 and neuronal injury. *Nat Rev Immunol*. 2005;5:629–640. doi: 10.1038/nri1664.
54. Whiteley W, Jackson C, Lewis S, Lowe G, Rumley A, Sandercock P, et al. Inflammatory markers and poor outcome after stroke: a prospective cohort study and systematic review of interleukin-6. *PLoS Med*. 2009;6:e1000145. doi: 10.1371/journal.pmed.1000145.
55. McCoy MK, Tansey MG. TNF signaling inhibition in the CNS: implications for normal brain function and neurodegenerative disease. *J Neuroinflammation*. 2008;5:45. doi: 10.1186/1742-2094-5-45.
56. Ohtaki H, Ylostalo JH, Foraker JE, Robinson AP, Reger RL, Shioda S, et al. Stem/progenitor cells from bone marrow decrease neuronal death in global ischemia by modulation of inflammatory/immune responses. *Proc Natl Acad Sci U S A*. 2008;105:14638–14643. doi: 10.1073/pnas.0803670105.
57. Le Blanc K, Ringdén O. Immunomodulation by mesenchymal stem cells and clinical experience. *J Intern Med*. 2007;262:509–525. doi: 10.1111/j.1365-2796.2007.01844.x.
58. Aggarwal S, Pittenger MF. Human mesenchymal stem cells modulate allogeneic immune cell responses. *Blood*. 2005;105:1815–1822. doi: 10.1182/blood-2004-04-1559.
59. Uccelli A, Pistoia V, Moretta L. Mesenchymal stem cells: a new strategy for immunosuppression? *Trends Immunol*. 2007;28:219–226. doi: 10.1016/j.it.2007.03.001.
60. Ren G, Zhang L, Zhao X, Xu G, Zhang Y, Roberts AI, et al. Mesenchymal stem cell-mediated immunosuppression occurs via concerted action of chemokines and nitric oxide. *Cell Stem Cell*. 2008;2:141–150. doi: 10.1016/j.stem.2007.11.014.
61. Ortiz LA, Dutreil M, Fattman C, Pandey AC, Torres G, Go K, et al. Interleukin 1 receptor antagonist mediates the antiinflammatory and antifibrotic effect of mesenchymal stem cells during lung injury. *Proc Natl Acad Sci U S A*. 2007;104:11002–11007. doi: 10.1073/pnas.0704421104.
62. Borlongan CV, Hadman M, Sanberg CD, Sanberg PR. Central nervous system entry of peripherally injected umbilical cord blood cells is not required for neuroprotection in stroke. *Stroke*. 2004;35:2385–2389. doi: 10.1161/01.STR.0000141680.49960.d7.
63. Uccelli A, Moretta L, Pistoia V. Mesenchymal stem cells in health and disease. *Nat Rev Immunol*. 2008;8:726–736. doi: 10.1038/nri2395.
64. Shen LH, Li Y, Chen J, Zacharek A, Gao Q, Kapke A, et al. Therapeutic benefit of bone marrow stromal cells administered 1 month after stroke. *J Cereb Blood Flow Metab*. 2007;27:6–13. doi: 10.1038/sj.jcbfm.9600311.
65. Bang OY, Lee JS, Lee PH, Lee G. Autologous mesenchymal stem cell transplantation in stroke patients. *Ann Neurol*. 2005;57:874–882. doi: 10.1002/ana.20501.
66. Mitkari B, Nitzsche F, Kerkelä E, Kuptsova K, Huttunen J, Nystedt J, et al. Human bone marrow mesenchymal stem/stromal cells produce efficient localization in the brain and enhanced angiogenesis after intra-arterial delivery in rats with cerebral ischemia, but this is not translated to behavioral recovery. *Behav Brain Res*. 2014;259:50–59. doi: 10.1016/j.bbr.2013.10.030.
67. Steiner B, Roch M, Holtkamp N, Kurtz A. Systemically administered human bone marrow-derived mesenchymal stem home into peripheral organs but do not induce neuroprotective effects in the MCAo-mouse model for cerebral ischemia. *Neurosci Lett*. 2012;513:25–30. doi: 10.1016/j.neulet.2012.01.078.
68. Wang LQ, Lin ZZ, Zhang HX, Shao B, Xiao L, Jiang HG, et al. Timing and dose regimens of marrow mesenchymal stem cell transplantation affect the outcomes and neuroinflammatory response after ischemic stroke. *CNS Neurosci Ther*. 2014;20:317–326. doi: 10.1111/cns.12216.